

Collisional Quenching and Vibrational Energy Transfer in the $A^2\Sigma^+$ Electronic State of the CF Radical

Boris Nizamov and Paul J. Dagdigian*

Department of Chemistry, The Johns Hopkins University, Baltimore, Maryland 21218-2685

Received: July 27, 2000; In Final Form: October 18, 2000

Electronic quenching of the $v' = 0$ and 1 vibrational levels and $v' = 1 \rightarrow v' = 0$ vibrational energy transfer has been studied at room temperature for the $A^2\Sigma^+$ electronic state of the CF radical. The colliders investigated were He, Ar, H₂, N₂, CH₄, O₂, CO, C₃H₈, and CF₄. Room-temperature thermal rate constants were determined. With the exception of CF₄, the quenching rate constants were significant for all molecular colliders. Vibrational energy transfer within the $A^2\Sigma^+$ state was observed only for the CH₄ collision partner.

1. Introduction

Absolute concentrations of molecular free radicals have been widely measured in flames,^{1,2} plasmas,³ the troposphere,⁴ and other collisional environments by laser-induced fluorescence. Since collisions within the radiative lifetime of the excited state can remove molecules from the initially excited level by electronic quenching or collisional energy transfer to other rovibrational levels in the excited state, knowledge of these rate constants is crucial for the determination of species concentrations from the measured fluorescence intensities. We report here a study of collisional quenching and vibrational energy transfer of the $A^2\Sigma^+$ electronic state of the CF radical.

The CF radical occurs in plasmas which are used for etching SiO₂ layers in the fabrication of microelectronic circuits and which employ CF₄ and other partially or fully fluorinated hydrocarbons. This radical also is important in the chemistry of flames containing fluorinated hydrocarbons.⁵ The CF radical is conveniently detected by its $A^2\Sigma^+ - X^2\Pi$ electronic transition, whose origin band lies near 233 nm.^{6–8} The $v' = 0$ and 1 vibrational levels decay radiatively, while only weak fluorescence has been detected from the $v' = 2$ level, indicative of excited-state predissociation.⁹ Recently, the $A - X(2,0)$ band was recorded with good signal-to-noise ratio in an rf plasma by cavity ring-down spectroscopy.¹⁰ On the basis of ab initio potential energy curves,¹¹ as well as experimental values for the ground-state dissociation energy¹² and the excitation energies of the $A^2\Sigma^+$ and $a^4\Sigma^-$ states,^{8,13} Booth et al.⁹ conclude that the predissociation is consistent with tunneling through a barrier in the $A^2\Sigma^+$ state. A theoretical study of the predissociation of the lower-lying electronic states of CF has recently been carried out.¹⁴ The computed predissociation rates for the rovibrational levels of the $A^2\Sigma^+$ state are consistent with the above-described observations.

Radiative lifetimes of the $v' = 0$ and 1 vibrational levels of CF($A^2\Sigma^+$) have been measured by following the fluorescence decay after pulsed laser excitation.¹⁵ The lifetimes of these levels are relatively short: 26.7 ± 1.8 and 25.6 ± 1.8 ns, respectively. Earlier measurements of the radiative lifetime, obtained by following the time-resolved emission after pulsed electron impact excitation of fluorinated hydrocarbons^{16,17} or from measurement of the transition dipole moment in a shock tube,¹⁸ yielded somewhat shorter lifetimes. Relative transition probabilities for specific (v', v'') bands in the $A - X$ system were

measured for the $v' = 0$ and 1 levels and were employed to deduce the radial dependence of the transition dipole moment.⁹

To our knowledge, collisional quenching rate constants have not been previously reported for the CF($A^2\Sigma^+$) excited electronic state. Concentration profiles of CF have been measured in rf plasmas by laser-induced fluorescence,^{3,19–23} as well as absorption-based techniques, including UV absorption,²⁴ UV cavity ring-down spectroscopy,¹⁰ and infrared diode laser absorption.^{25,26} These spectroscopic diagnostic techniques largely employ the $A^2\Sigma^+ - X^2\Pi$ electronic transition. The total pressure in these plasmas was 50–500 mTorr. Because of the short CF($A^2\Sigma^+, v'$) radiative lifetimes, the reduction of the excited-state lifetimes by electronic quenching is relatively small, and CF concentrations could be reliably deduced from the fluorescence signals without correction for collisional loss in the excited state. At higher pressure, such as an atmospheric-pressure flame, electronic quenching and other collisional processes will, however, be important.

In this paper, rate constants for electronic quenching of the $v' = 0$ and 1 vibrational levels of CF($A^2\Sigma^+$) with a number of molecular colliders are reported. Quenching by He and Ar was also investigated, and upper bounds to collisional quenching by these atoms are reported. Collisional $v' = 1 \rightarrow v' = 0$ vibrational energy transfer was also investigated. This process was detected only for CH₄ collision partner. The study of electronic quenching and vibrational energy transfer in CF($A^2\Sigma^+$) is also of interest from the viewpoint of collision dynamics. Such processes have been extensively studied for a number of diatomic free radicals of importance in combustion and other reacting environments.

2. Experimental Section

CF radicals were produced by photolysis of CFCl₃ at 193 nm in a cell consisting of a central chamber with opposing sidearms for entry and exit of the photolysis and excitation laser beams. The CFCl₃ precursor (Aldrich, 99+%) was admitted into the central chamber about 15 cm upstream from the observation zone. The collider gas was introduced through the ends of the sidearms, and the gas mixture was slowly flowed through the cell. The total pressure was in the range 0.3–35 Torr depending on the experiment, while the partial pressure of CFCl₃ was typically ~ 5 mTorr. The purity of the He, Ar, H₂, and N₂ reagents was better than 99.997%, the purity of CH₄ was

99.99%, and the purity of O₂, CO, C₃H₈, and CF₄ was better than 99.5%. The absolute pressure was monitored with a capacitance manometer (MKS).

The 193 nm output of a COMPLEX 102 (Lambda Physik) ArF excimer laser was focused using a 1-meter lens above the slit of a 1-meter *f*/9 Fastie-Ebert spectrometer with 8 Å/mm dispersion in the first order. For fluorescence decay waveform measurements, the spectrometer slits were opened wide enough to collect emission from all rotational lines of the vibrational level under investigation. The typical pulse energy of the excimer laser in the vacuum chamber was ~20 mJ. The excitation laser beam (~4 mm in diameter) was introduced through the opposite sidearm and had a spectral full width at half-maximum (fwhm) of 0.4 cm⁻¹ and temporal fwhm of 6 ns. The energy of the excitation laser was about 300 μJ. The delay (controlled by a digital delay generator) between the photolysis and the excitation lasers was 30 μs. The delay between the photolysis and excitation lasers was long enough to allow thermalization of the CF radicals to a room-temperature velocity distribution and to allow emission from the excited electronic states produced by photolysis to decay away.

Fluorescence was detected with two separate photomultiplier (PMT) detectors. A Hamamatsu R928 PMT was placed at the exit slit of the spectrometer and was used to collect waveforms or to record wavelength-resolved fluorescence emission spectra. The second PMT (EMI Thorn 9813QB) was used to monitor the total fluorescence signal from the excited upper-state level. The latter detector allowed us to check for variations in the concentration of CF radicals due to changes in the partial pressure of the CFCI₃ precursor and/or the 193 nm laser energy.

The transient signals from the PMTs were directed to a digital oscilloscope or gated integrators (Stanford Research Systems SR250), and their outputs were collected under computer control and stored on magnetic media for later analysis. The Hamamatsu R928 PMT had a rise time 2.2 ns, and Lecroy model 9360 digital scope used to digitize the waveforms had a bandwidth of 600 MHz. The typical sampling rate of the digital scope was 0.2–0.4 ns per point. For collection of the waveforms, the digital scope was triggered by scattered light from the excitation laser using a fast photodiode. Each waveform was averaged over 1000 laser shots to increase the dynamic range and signal-to-noise ratio. Background waveforms were collected with the excitation laser beam blocked and subtracted from the CF(A²Σ⁺, *v*' = 0, 1) fluorescence decay waveforms. Effects of saturation of the PMT were minimized by checking that the decay lifetimes were not artificially lengthened at the typical signal levels used for kinetic measurements.

3. Results

3.1. Excitation Spectra. Excitation spectra of the A²Σ⁺ – X²Π *v*' = 0, 1 ← *v*'' = 0 bands were recorded by scanning excitation laser wavelength and observing laser excited fluorescence through an interference filter with peak transmission at 254 nm and a band-pass of 20 nm. All rotational lines in the excitation spectra were identified as belonging to the A – X band system. Given an excellent signal-to-noise ratio in the excitation spectra, we conclude that all of the observed fluorescence was due to emission from laser-excited A²Π *v*' = 0, 1 levels. Photolysis of CFCI₃ precursor is a much cleaner source of CF radicals as compared to a discharge in CF₄, since the latter also produces CF₂, which has an electronic transition in the same wavelength range as the CF A – X band system. Absence of interfering emission is important for accurate measurement of short fluorescence decay lifetimes.

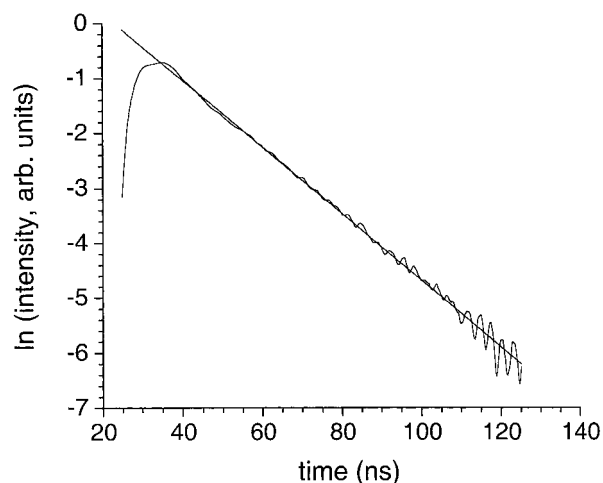


Figure 1. A semilogarithmic plot of the fluorescence decay of CF(A²Π, *v*' = 0) in the presence of 15 Torr hydrogen. The straight line is a least-squares fit to the decay, as described in the text.

3.2. Collisional Electronic Quenching Rate Constants.

Waveforms of the fluorescence decay from the laser-excited A²Π *v*' = 0, 1 levels were recorded at different pressures of the atomic and molecular colliders He, Ar, CF₄, CH₄, N₂, O₂, CO, H₂, and C₃H₈. The excitation laser was tuned to the band heads in either the *P*₁₂ or *P*₁₁ branches of the (0,0) or (1,0) bands.⁸ No systematic difference in the measured decay rate constants was observed when different band heads were used for excitation of the same *v*' vibrational level. Excitation in these band heads is appropriate for the measurement of quenching rate constants. The heads in the *P*₁₁ and *P*₁₂ branches occur at essentially the same rotational angular momentum *J*, which moreover corresponds to the maximum population in a room-temperature Boltzmann distribution.

Fluorescence from the excited *v*' = 0 and 1 vibrational levels was monitored by observing emission in the (0,2) and (1,0) bands, respectively. For all quenching gases the semilogarithmic plots of the waveforms were linear to within our experimental uncertainties over the first four decay lifetimes, and the decays thus appeared to be single exponential. An example of our observed waveforms is shown in Figure 1. The decay waveforms were fit over first three to four decay time constants starting ~40 ns after the laser pulse. The time range over which waveforms could be fit was not limited by the signal-to-noise ratio but rather by a PMT after-pulse which occurred ~110 ns after the laser pulse.

Electronic quenching rate constants were determined from plots of the decay rates as a function of the collider gas pressure, such as those shown in Figure 2. The ranges of pressures investigated for these plots were chosen such that the first-order decay constant increased by a factor of 1.7 to 2.5 times the rate constant for purely radiative decay, except for those colliders for which the collisional quenching rate constants were small. For each quenching gas and *v*' vibrational level, 2–4 plots were used to determine the quenching rate constant and to estimate the statistical errors. The derived quenching rate constants are presented in Table 1. By averaging the zero-pressure intercepts of the decay-rate plots, we obtain radiative lifetimes of 26.4 ± 2.0 and 25.7 ± 2.0 ns for the CF(A²Σ⁺) *v*' = 0 and 1 vibrational levels, respectively. These values are in excellent agreement with those reported by Booth and Hancock.¹⁵

We found that CF₄ did not quench CF(A²Σ⁺, *v*' = 1) to a significant degree over the 0–20 Torr pressure range; consequently, we did not investigate the quenching of the *v*' = 0

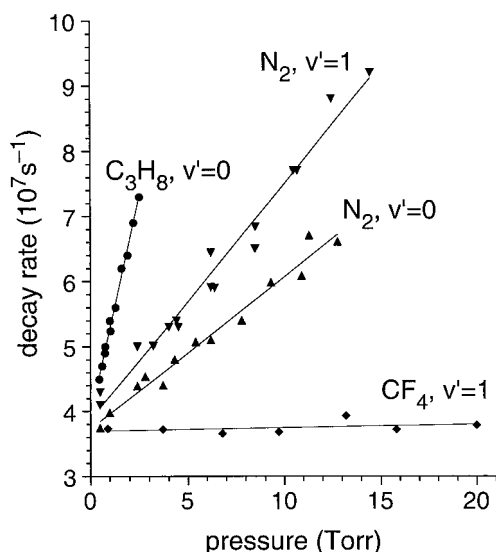


Figure 2. Plots of the CF(A²Π, *v'*) decay rates as a function of the collider gas pressure. A subset of the data collected for the determination of the quenching rate constants reported in Table 1 is presented in the figure.

TABLE 1: Rate Constants k_q (Units: 10^{-10} Molecule⁻¹ cm³ s⁻¹) and Cross Sections σ_q (Units: Å²) for Total Collisional Removal of the CF A²Σ⁺ *v'* Vibrational Levels

collider	k_q		σ_q^a	
	<i>v'</i> = 0	<i>v'</i> = 1	<i>v'</i> = 0	<i>v'</i> = 1
H ₂	0.24 ± 0.04	0.40 ± 0.05	1.3 ± 0.2	2.2 ± 0.3
N ₂	0.69 ± 0.08	1.11 ± 0.12	10.5 ± 1.2	17.0 ± 1.8
O ₂	1.59 ± 0.23	1.80 ± 0.18	25.1 ± 3.6	28.5 ± 2.9
CO	2.13 ± 0.38	2.74 ± 0.28	32.5 ± 5.8	41.8 ± 4.3
CH ₄	0.40 ± 0.09	1.21 ± 0.11	5.2 ± 0.2	16.6 ± 1.5
C ₃ H ₈	4.6 ± 0.6	7.7 ± 1.0	68 ± 9	130 ± 17
CF ₄	<i>b</i>	<0.04		
He	<0.04	<0.04		
Ar	<0.04	<0.04		

^a Computed from the rate constants k_q by dividing by the mean relative velocity $\bar{v} = (8kT/\pi\mu)^{1/2}$, where μ is the collision reduced mass.

^b Not measured.

level by CF₄. We also did not observe collisional quenching of the *v'* = 0 and 1 vibrational levels by He and Ar for pressures up to 35 Torr. Strictly speaking, the measured rate constants for *v'* = 1 are total removal rate constants and include collisional vibrational energy transfer and electronic quenching. The former process is considered in detail in the section below.

3.3. Collisional Vibrational Energy Transfer. Collisional vibrational energy transfer (VET) in CF(A²Σ⁺) from *v'* = 1 to *v'* = 0 was investigated by recording resolved fluorescence spectra following laser excitation of the *v'* = 1 vibrational level. The collider pressure for such scans was chosen such that the *v'* = 1 collisional quenching rate would approximately equal the purely radiative decay rate, with the exception of the weakly quenching colliders He, Ar, and CF₄, for which emission spectra were recorded at pressures of ~30 Torr. The emission spectra were recorded in a time window of 0–200 ns after the laser pulse.

Emission from the collisionally populated *v'* = 0 level was observed only for CH₄ collider gas. In this case, it was possible to determine the bimolecular rate constant for *v'* = 1 → *v'* = 0 VET. For the other collision partners, only an upper estimate of the VET rate constant could be estimated from the signal-to-noise ratio in the spectra and the pressure at which these spectra were recorded.

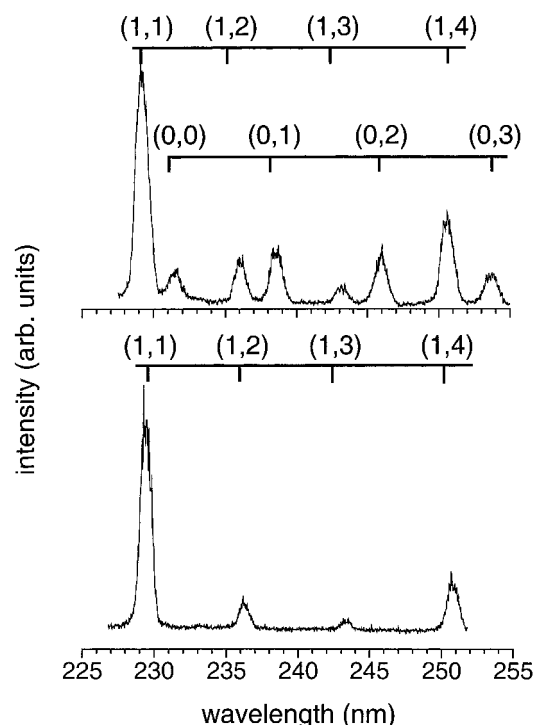


Figure 3. CF A²Σ⁺ - X²Π emission spectra following excitation of *v'* = 1 in the presence of (a) 6.0 Torr CH₄, and (b) 30 Torr He. The (*v'*, *v''*) bands are marked.

Figure 3 displays emission spectra following excitation of *v'* = 1 in CH₄ and He, recorded at 6.0 and 30 Torr, respectively. It is obvious that VET is much more efficient in CH₄ than in He, as emission from *v'* = 0 is clearly observed for CH₄ collider but *v'* = 0 bands are absent for He. To determine the rate constant for VET, fluorescence decay waveforms for *v'* = 1 and 0 were recorded by following the time-dependent emission in the (1,1) and (0,2) bands, respectively. The relative intensities in these two bands were converted to relative populations of the *v'* = 0 and 1 vibrational levels using the (*v'*, *v''*) band strengths reported by Booth et al.⁹ It should be noted that the relative intensities of the (1, *v''*) and (0, *v''*) bands as a function of the lower-state vibrational quantum number *v''* are in good agreement with the vibrationally resolved emission spectra reported by Booth et al.⁹

The rate constant for *v'* = 1 → *v'* = 0 VET was determined from the time-dependent *v'* = 0 and 1 relative vibrational populations with the following kinetic model. The *v'* = 1 → *v'* = 0 VET process can be considered as irreversible since at room temperature $kT = 208$ cm⁻¹ is much smaller than the *v'* = 1 to 0 vibrational interval⁸ $\Delta G_{1/2} = 1719$ cm⁻¹. Hence, the decay of the *v'* = 1 level is expected to be exponential, as was observed. Neglecting the reverse *v'* = 0 → *v'* = 1 VET process, the rate equation for the *v'* = 0 level can be written as

$$dN_0/dt = k_{\text{vib}}nN_1 - (k_{\text{rad}} + k_qn)N_0 \quad (1)$$

where N_0 and N_1 are the populations of the *v'* = 0 and 1 vibrational levels, n is the density of the collider, k_{vib} is *v'* = 1 → *v'* = 0 VET rate constant to be determined, and k_q is the quenching rate constant for *v'* = 0, which was taken from Table 1. The experimentally measured waveform for the *v'* = 1 level was used to describe the time dependence of the population N_1 , and k_{vib} was varied to obtain the best agreement between the experimentally measured waveform for *v'* = 0 and the solution of eq 1. For measurements made at 4.6 and 6.0 Torr

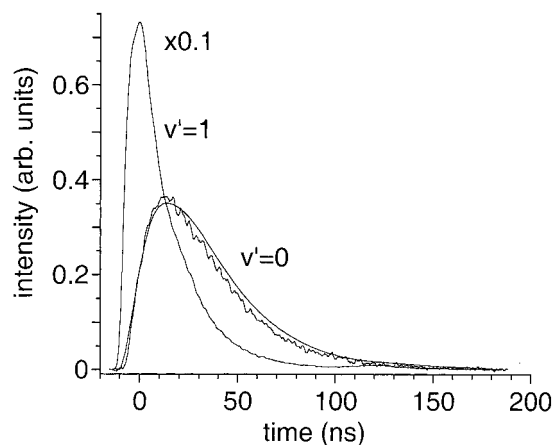


Figure 4. Waveforms of the emission from the $\text{CF}(A^2\Pi)$ $v' = 0$ and 1 vibrational levels with laser excitation of the $v' = 1$ level. These waveforms were collected at 4.6 Torr CH_4 . The smooth curve represents a fit to the $v' = 0$ waveform with eq 1.

of CH_4 , the best agreement between the experimental and simulated waveforms was obtained for $k_{\text{vib}} = 3.3 \times 10^{-11} \text{ molecule}^{-1} \text{ cm}^3 \text{ s}^{-1}$, with an estimated uncertainty of $\pm 0.4 \times 10^{-11} \text{ molecule}^{-1} \text{ cm}^3 \text{ s}^{-1}$. This VET rate constant is $\sim 27\%$ of the corresponding total removal rate constant for the $v' = 1$ level, given in Table 1. An example of the experimental and simulated waveforms is given in Figure 4.

For the collision partners other than CH_4 , only an upper limit to the VET rate constant could be obtained. The typical signal-to-noise ratio in the emission spectra was about 100:1. Assuming that the $v' = 0$ VET signal was less than the noise level, one can estimate that the first-order VET rate constant was less than 1% of the total decay rate constant. For He, Ar, and CF_4 an upper estimate of the $v' = 1 \rightarrow v' = 0$ VET rate constant is $0.04 \times 10^{-11} \text{ molecule}^{-1} \text{ cm}^3 \text{ s}^{-1}$. For propane, the VET rate constant is less than $0.6 \times 10^{-11} \text{ molecule}^{-1} \text{ cm}^3 \text{ s}^{-1}$, while for the rest of the collision partners an upper estimate of the VET rate constant is somewhere between these two values. Hence, for all colliders except CH_4 , the $v' = 0$ and 1 rate constants reported in Table 1 refer to the electronic quenching process only.

4. Discussion

The rate constants for the electronic quenching of electronically excited $\text{CF}(A^2\Sigma^+)$ are seen in Table 1 to vary widely for the different collider gases. The largest rate constants involve the molecular colliders C_3H_8 , CO, and O_2 . Significantly smaller rate constants were found for the N_2 , CH_4 , and H_2 colliders. The rate constants for the monatomic collision partners $\text{M} = \text{He}$ and Ar, and also CF_4 , were too small to be measured. These small rate constants imply that the ground and excited potential energy surfaces correlating with the asymptotic $\text{CF}(X)$ and $\text{CF}(A)$ states do not cross at thermally accessible translational energies in $\text{CF}(A) + \text{M}$ collisions.

It is of interest to compare our rate constants for the electronic quenching of $\text{CF}(A^2\Sigma^+)$ with the rate constants for the quenching of the first excited state ($A^2\Delta$) of the isovalent CH radical. With the exception of CF_4 , room-temperature rate constants for the electronic quenching of $\text{CH}(A^2\Delta, v' = 0)$ are available in the literature.^{27–32} A similar ordering of the values of the $\text{CF}(A^2\Sigma^+, v' = 0)$ and $\text{CH}(A^2\Delta, v' = 0)$ electronic quenching rate constants are found. The most significant difference is that the rate constant for $\text{CH}(A^2\Delta)$ quenching by N_2 is very small³⁰ [$(2.2 \pm 0.6) \times 10^{-13} \text{ molecule}^{-1} \text{ cm}^3 \text{ s}^{-1}$], which contrasts with the

significant magnitude of the rate constant reported in Table 1 for $\text{CF}(A^2\Sigma^+)$ quenching by N_2 .

The negligible rate constant for electronic quenching of $\text{CF}(A^2\Sigma^+)$ by the molecular gas CF_4 is quite surprising. However, a very small rate constant [$3 \times 10^{-12} \text{ molecule}^{-1} \text{ cm}^3 \text{ s}^{-1}$] was also found for the quenching of $\text{CF}_2(\tilde{A}^1B_1(0,6,0))$ by CF_4 .³³ The quenching rate constants of this species by hydrocarbons³⁴ show trends similar to what we have observed for $\text{CF}(A^2\Sigma^+)$, but the magnitudes are slightly smaller, e.g. $k(\text{CF}_2(\tilde{A})-\text{CH}_4) = (1.0 \pm 0.5) \times 10^{-11} \text{ molecule}^{-1} \text{ cm}^3 \text{ s}^{-1}$ and $k(\text{CF}_2(\tilde{A})-\text{C}_3\text{H}_8) = (1.1 \pm 0.2) \times 10^{-10} \text{ molecule}^{-1} \text{ cm}^3 \text{ s}^{-1}$.

For all colliders for which nonnegligible quenching rate constants could be measured for $\text{CF}(A^2\Sigma^+)$, the values for the $v' = 1$ level were larger than for $v' = 0$. Strictly speaking, the rate constants for $v' = 1$ include two possible removal processes, electronic quenching and $v' = 1 \rightarrow v' = 0$ vibrational energy transfer. For some colliders, the increase in the rate constant for $v' = 1$ over that for $v' = 0$ was relatively modest, e.g. 13% and 29% for O_2 and CO, respectively, while the increase in the total removal rate constant was $\sim 65\%$ for N_2 , H_2 , and C_3H_8 . A very dramatic increase, approximately a factor of 3, in the total removal rate constant for $v' = 1$ as compared to that for $v' = 0$ was found for CH_4 collider.

To determine what fraction of the increased total removal rate constant for $v' = 1$ can be attributed to VET, we recorded spectrally resolved emission spectra for excitation of $v' = 1$ and thus observed the collisional formation of the $v' = 0$ level as the initially excited $v' = 1$ population decays. Vibrational energy transfer could be observed only for collisions with CH_4 . In this case, VET accounts for only $\sim 40\%$ of the increase of the total removal rate constant for $v' = 1$ over that for $v' = 0$. Thus, for all the colliders most, if not all, of the increase in the total removal rate for $v' = 1$ as compared with that for $v' = 0$ can be ascribed to an increase in the rate of electronic quenching, and not to the opening of the VET channel.

As noted in the Introduction, the $v' = 2$ level of $\text{CF}(A^2\Sigma^+)$ is subject to predissociation, because of tunneling through a barrier in the excited-state potential energy curve. It is possible that the differing quenching behavior of the $v' = 0$ and 1 levels is related to this barrier in the potential energy curve, as the enhanced $v' = 1$ quenching may involve collision-induced predissociation. The potential energy curve of the $\text{CH}(B^2\Sigma^-)$ state also possesses a barrier, and only the $v' = 0$ and 1 level radiatively decay.³⁵ It is possible that there is a similar enhancement of the electronic quenching rates for the $v' = 1$ level of this radical. Unfortunately, to our knowledge the quenching of $v' = 0$ only has been studied for the $\text{CH}(B^2\Sigma^-)$ state.^{36–38}

A facile mechanism for vibrational energy transfer is resonant $V - V$ transfer to the collider gas.³⁹ This mechanism would not be expected to be operative for the diatomic colliders since their vibrational intervals are significantly larger than the $\text{CF}(A^2\Sigma^+)$ interval, given above. Methane has an infrared-active degenerate bending mode, of frequency 1306 cm^{-1} .⁴⁰ This could be an suitable acceptor mode, especially if additional energy were taken up by rotation. By contrast, CF_4 has a suitable acceptor mode of similar frequency, and propane has a number of suitable acceptor modes with closer frequency matches to CF; however, no VET was detected for these colliders.

For all colliders for which total removal rate constants could be measured, Table 1 also presents estimated cross sections, obtained by dividing the rate constants by the mean relative velocity. It can be seen that the magnitudes of some of these cross sections are substantial. This suggests that attractive forces

are playing a role in the collision dynamics. Several simplified models have been invoked to rationalize the magnitudes of quenching and energy transfer cross sections.

Parmenter and co-workers⁴¹ advanced a model in which the magnitude of the attractive interaction between the electronically excited diatom and the collider would govern the magnitude of the cross section. This model proposes the following relationship between the cross section σ and the Lennard-Jones well-depth ϵ_{A^*M} of the attractive potential well of the interaction between the excited molecule A* and the collider M:

$$\ln \sigma = \ln C + \epsilon_{A^*M}/kT \quad (2)$$

where C is a constant. Since such well depths are generally unknown, ϵ_{A^*M} is approximated as the geometric mean of the well depths $\epsilon_{A^*A^*}$ and ϵ_{MM} . Since the latter are available,⁴² we obtain the following predicted correlation:

$$\ln \sigma = \ln C + \beta \sqrt{\epsilon_{MM}/k} \quad (3)$$

where $\beta = [\epsilon_{A^*A^*}/kT^2]^{1/2}$. Equation 3 has been found to yield a reasonable correlation for the room-temperature quenching rate cross sections of OH(A²Σ⁺)^{43,44} and NH(c¹Π),⁴⁵ but this relationship does not predict well the temperature dependence of an individual quenching cross section. In the case of CH(A²Δ), the room-temperature quenching cross sections are not fitted well by such a model.³² Similarly, the cross sections reported in Table 1 fit the correlation predicted by eq 3 very poorly.

Other models have been developed to interpret quenching cross sections. These include a simple collision complex capture trajectory calculation based on a one-dimensional attractive curve computed by an angular average of the long-range interactions.⁴³ Paul and co-workers have presented a harpoon model for the quenching of NO(A²Σ⁺) and OH(A²Σ⁺).^{46,47} This model considers the crossing of ionic potential energy curves with curves correlating with the excited diatomic state. Thus, important ingredients in this model are the electron affinity of the diatom and the ionization potential of the collider. The latter may provide an explanation of the small observed electronic quenching rate constants for CF(A²Σ⁺) [Table 1], CF₂(\tilde{A}^1B_1), and also OH(A²Σ⁺)⁴⁸ by CF₄ since the stable positive ion is not accessible by a vertical transition from neutral CF₄.

As anticipated previously³ for the short radiative lifetime of CF(A²Σ⁺), our measured rate constants for electronic quenching imply that the concentrations measured by laser-induced fluorescence in an rf plasma do not require significant correction for most colliders for collisional removal of the excited state at the low pressures (50–500 mTorr) in such reactors. By contrast, such corrections will be very important for measurements of the CF concentration in atmosphere-pressure flames.

Acknowledgment. We gratefully acknowledge John Doering for the loan of a 1 m Fastie-Ebert spectrometer. This work was supported by the U.S. Army Research Office (ARO), under Grant DAAG55-98-1-0312. The acquisition of the excimer laser was funded through ARO Grant DAAD19-00-1-0022.

References and Notes

- Eckbreth, A. C. *Laser Diagnostics for Combustion Temperature and Species Measurements*; Abacus Press: Tunbridge Wells, 1988.
- Kohse-Höinghaus, K. *Prog. Energy Combust. Sci.* **1994**, *20*, 203.
- Booth, J. P.; Cunge, G.; Chabert, P.; Sadeghi, N. *J. Appl. Phys.* **1999**, *85*, 3097; and references therein.
- Crosley, D. R. In *Current Problems and Progress in Atmospheric Chemistry*; Barker, J. R., Ed.; World Scientific: Singapore, 1996; p 256.
- Burgess, D. R. F.; Zachariah, M. R.; Tsang, W.; Westmoreland, P. R. In *Halon Replacements: Technology and Science*; Miziolek, A. W., Tsang, W., Eds.; ACS Symposium Series 611; American Chemical Society: Washington, DC, 1995; p 322.
- Andrews, E. B.; Barrow, R. F. *Nature* **1950**, *165*, 890.
- Andrews, E. B.; Barrow, R. F. *Proc. Phys. Soc. London* **1950**, *A64*, 481.
- Porter, T. L.; Mann, D. E.; Acquista, N. *J. Mol. Spectrosc.* **1965**, *16*, 228.
- Booth, J. P.; Hancock, G.; Toogood, M. J.; McKendrick, K. G. *J. Phys. Chem.* **1996**, *100*, 47.
- Booth, J. P.; Cunge, G.; Biennier, L.; Romanini, D.; and K. A. *Chem. Phys. Lett.* **2000**, *317*, 631.
- Rendell, A. P.; Bauschlicher, C. W., Jr.; Langhoff, S. R. *Chem. Phys. Lett.* **1989**, *163*, 354.
- Hildebrand, D. L. *Chem. Phys. Lett.* **1975**, *32*, 523.
- Grieman, F. J.; Droegge, A. T.; Engelking, P. C. *J. Chem. Phys.* **1983**, *78*, 2248.
- Petsalakis, I. D. *J. Chem. Phys.* **1999**, *110*, 10730.
- Booth, J. B.; Hancock, G. *Chem. Phys. Lett.* **1988**, *150*, 457.
- Hesser, J. E. *J. Chem. Phys.* **1968**, *48*, 2518.
- van Sprang, H. A.; Brongersma, H. H.; de Heer, F. J. *Chem. Phys.* **1978**, *35*, 51.
- Harrington, J.; Modica, A. P.; Libby, D. R. *J. Chem. Phys.* **1966**, *45*, 2720.
- Booth, J. P.; Hancock, G.; Perry, N. D. *Appl. Phys. Lett.* **1987**, *50*, 318.
- Hansen, S. G.; Luckman, G.; Colson, S. D. *Appl. Phys. Lett.* **1988**, *53*, 1508.
- Booth, J. P.; Hancock, G.; Perry, N. D.; Toogood, M. J. *J. Appl. Phys.* **1989**, *66*, 5251.
- Hansen, S. G.; Luckman, G.; Nieman, G. C.; Colson, S. D. *J. Vac. Sci. Technol. B* **1990**, *8*, 128.
- Conner, W. T.; Sawin, H. H. *Appl. Phys. Lett.* **1992**, *60*, 557.
- Booth, J. P.; Cunge, G.; Neuilly, F.; Sadeghi, N. *Plasma Sources Sci. Technol.* **1998**, *7*, 423.
- Haverlag, M.; Stoffels, W. W.; Stoffels, F.; Kroesen, G. M. W.; de Hoog, F. J. *J. Vac. Sci. Technol. A* **1996**, *14*, 384.
- Maruyama, K.; Ohkouchi, K.; Goto, T. *Jpn. J. Appl. Phys. Part 1* **1996**, *35*, 4081.
- Garland, N. L.; Crosley, D. R. *Chem. Phys. Lett.* **1987**, *134*, 189.
- Hontzopoulos, E.; Vlahoyannis, Y. P.; Fotakis, C. *Chem. Phys. Lett.* **1988**, *147*, 1321.
- Heinrich, P.; Kenner, R. D.; Stuhl, F. *Chem. Phys. Lett.* **1988**, *147*, 575.
- Kenner, R. D.; Pfannenber, S.; Heinrich, P.; Stuhl, F. *J. Phys. Chem.* **1991**, *95*, 6585.
- Chen, C.; Sheng, Y.; Yu, S.; Ma, X. *J. Chem. Phys.* **1994**, *101*, 5727.
- Cerezo, C.; Martin, M. *J. Photochem. Photobiol. A* **2000**, *134*, 127.
- Hack, W.; Langel, W. *J. Photochem.* **1983**, *21*, 105.
- Hack, W.; Langel, W. *J. Phys. Chem.* **1983**, *87*, 3462.
- Bernath, P. F.; Brazier, C. R.; Olsen, T.; Hailey, R.; Fernando, W. T. M. L. *J. Mol. Spectrosc.* **1991**, *147*, 16.
- Couris, S.; Anastopoulou, N.; Fotakis, C. *Chem. Phys. Lett.* **1988**, *147*, 321.
- Cooper, J. L.; Whitehead, J. C. *J. Chem. Soc., Faraday Trans.* **1992**, *89*, 1287.
- Rensberger, K. L.; Dyer, M. J.; Copeland, R. A. *Appl. Opt.* **1988**, *27*, 3679.
- Yardley, J. T. *Introduction to Molecular Energy Transfer*; Academic: New York, 1980.
- Shimanouchi, T. *Tables of Molecular Vibrational Frequencies*; Natl. Bur. Stand.: Washington, DC, 1972.
- Lin, H. M.; Seaver, M.; Tang, K. Y.; Knight, A. E. W.; Parmenter, C. S. *J. Chem. Phys.* **1979**, *70*, 5442.
- Hirschfelder, J. O.; Curtiss, C. F.; Bird, R. B. *Molecular Theory of Gases and Liquids*; Wiley: New York, 1954.
- Fairchild, P. W.; Smith, G. P.; Crosley, D. R. *J. Chem. Phys.* **1983**, *79*, 1795.
- Heard, D. E.; Henderson, D. A. *Phys. Chem. Chem. Phys.* **2000**, *2*, 67.
- Kenner, R. D.; Rohrer, F.; Stuhl, F. *J. Phys. Chem.* **1989**, *93*, 7824.
- Paul, P. H.; Gray, J. A.; Durant, J. L., Jr.; Thoman, J. W., Jr. *Appl. Phys. B* **1993**, *57*, 249.
- Paul, P. H. *J. Quant. Spectrosc. Radiat. Transfer* **1994**, *51*, 511.
- Wysong, I. J.; Jeffries, J. B.; Crosley, D. R. *J. Chem. Phys.* **1990**, *92*, 5218.